Available online at www.sciencedirect.com

SCIENCE DIRECT®

Surface & Coatings Technology 200 (2006) 5614 – 5630

SURFACE & COATINGS TECHNOLOGY

www.elsevier.com/locate/surfcoat

The effect of multilayer filtered arc coatings on mechanical properties, corrosion resistance and performance of periodontal dental instruments

Vladimir Gorokhovsky [a,*], Brad Heckerman [a], Philip Watson [b], Nicholas Bekesch [c]

[a] *American Eagle Instruments, Inc., Missoula, MT, USA*
[b] *University of Toronto, Canada*
[c] *Dental Clinic, Ontario, Canada*

Received 21 October 2004; accepted in revised form 28 July 2005
Available online 3 October 2005

Abstract

A large-area filtered arc deposition (LAFAD) process was used to deposit various multi-layer cermet coatings on dental scalers made of martensitic stainless steel. A custom mechanical stroking device was used to include features capable of simulating the load and motion of dental scalers against enamel or dentin tooth surfaces in an aqueous environment. Subjecting the coated instruments to vibratory tumbling in a vat containing cellulose filler and an abrasive tested the abrasion resistance of the coating. The working edge wear was then investigated by means of optical and electron microscopy as well as by metallurgical cross-section profile analysis. Coating adhesion was determined by measuring delamination during Rockwell testing. Corrosion resistance of dental instruments with multi-layer coatings was studied by subjecting the instruments to repeated conventional autoclave sterilization procedures. Comparison of the laboratory tests with the field testing results in dental clinical practice is presented. The mass production yield of high-quality scalers with LAFAD coatings is discussed.

Keywords: Dental instruments; Coatings; Filtered arc; Multilayer; Superlattice; Ionitriding; Abrasive wear; Corrosion

1. Introduction

In dental therapeutics, most of the procedures, whether endodontic, restorative, periodontal, or surgical, involve interaction between cutting or scraping instruments and one of the hardest tissues of the animal kingdom.

In endodontics, the interaction is between the file and the dentine surrounding the canal, or occasionally, bone surrounding the tooth as in periapical surgery.
In restorative, the interaction is between the burs or hand instruments and dentine, enamel, precious metal alloys, amalgam, composite restorative materials, non-precious alloys of nickel and chromium, and porcelain.
In periodontics, the interaction is between scraping and/or cutting instruments and dentine, enamel and bone, calculus, and any restorative material and its margins that is attached to the tooth.
In oral surgery, the interaction is again between cutting and/or scraping instruments and bone, dentine, enamel, precious metal alloys, amalgam, composite restorative materials, non-precious alloys of nickel and chromium, and porcelain.

The instruments used are therefore made of tempered surgical or carbon steel and sometimes with ultra-hard inserts, of tungsten carbide, welded to the steel base. In every case, the use of these instruments is accompanied by varying degrees of wear. In order to compensate for this wear, the instruments are either replaced or re-sharpened. The maintenance of the sharp edge is extremely important since the sharp edge allows the operator to feel the texture and contour of the tooth or the root when direct visual examination is not possible, e.g., in sub-gingival scaling and root planing, and to estimate the hardness of the tooth material, e.g., when detecting decay, or when assessing if

* Corresponding author.
E-mail address: vigase@aol.com (V. Gorokhovsky).

0257-8972/$ - see front matter © 2005 Elsevier B.V. All rights reserved.
doi:10.1016/j.surfcoat.2005.07.104

the decay was adequately removed during restorative procedures.

Re-sharpening is usually done by stroking the instrument with an Arkansas, India and Ceramic stones of one of a number of different shapes. If the shape of the instrument is simple, this re-sharpening can be done relatively simply. If, however, the instrument has cutting surfaces that are curved, oriented in different planes (scalers and curettes), or if the cutting surfaces are designed to mate with an opposing surface (hemostats, scissors), this sharpening becomes very difficult. One can easily do irreparable damage to the instrument by the slightest miscalculation of angle or by a momentary lapse of attention. Also, the more intricate the shape of the instrument, the more time consuming is the sharpening process. There are numerous mechanical devices that have been created and patented to simplify the process but they are an aid and not a replacement for a well-trained operator. These sharpening aids are usually not automated and cannot take an instrument and automatically refinish the cutting edges. With the current labor costs, this time-consuming re-sharpening of instruments becomes more and more costly.

Even if the sharpening procedure takes a few minutes per instrument tip, the labor cost will outweigh the replacement cost of the instrument after only a few sharpening sequences. This does not take into account the loss of productivity by the dentist or hygienist. The constant re-sharpening of instruments has another, possibly more sinister, side effect. Every stroke of the sharpening stone removes a small amount of metal from the instrument. With repeated sharpening, the thinner parts of the instrument can become sufficiently weak to cause breakage during function creating a danger of the piece of metal's becoming imbedded in the surrounding tissue. Many instruments (especially scalers and curettes) are designed to be bulky in the beginning to minimize future fractures. When a well-polished instrument edge is re-sharpened, the sharpening stones invariably produce numerous striations on each of the contacted surfaces. These striations can be easily seen under relatively minor magnification. Fine oil-stone produces serrations that can be seen by the unaided eye. Arkansas stone, which is usually used for sharpening dental instruments, produces serrations, which are clearly visible under 10× magnification and are 10–20 μm in depth. The resulting cutting edge, therefore, becomes saw-like. When the root of the tooth is scraped with such edge, the serrations are transferred to the root surface. Since the bacteria responsible for tooth decay and for gum disease are about 0.2 μm, these serrations provide superb "hiding" places for them to attach and to replicate. If these iatrogenically produced serrations are supra-gingival, they can be reduced by polishing the tooth with a rotary rubber cup with a very mild abrasive. This procedure is known as "dental prophylaxis". Deep sub-gingival areas are protected from this polishing and may therefore become more susceptible to decay and to gum disease.

PVD cermet coating is known to enhance corrosion and wear resistance of the medical instruments [1–3,13–15]. It also eliminates any potential allergic reactions to the metal alloys by screening the substrate surface from the tissue [3]. This paper represents the results of an assessment of a novel large area filtered arc surface engineering technology's use in dentistry. This technology permits the scaler, curette, or other surgical instrument to be used for extended periods without re-sharpening. These instruments can therefore be manufactured to be more slender so that they can be introduced into confined spaces (e.g., periodontal pocket), with less trauma to surrounding tissue, and discomfort to the patient, while maintaining a long service life without the hassle of constant re-sharpening.

2. Experimental details

2.1. Substrate materials

Curettes and scalers of different shapes, all made of martensitic 440A stainless steel, were used as substrate materials. A photograph of one shape of dental scaler used in this work is shown in Fig. 1. Most of these instruments were manufactured by American Eagle Instrument, Inc. (AEI). Although instruments of other manufacturers were also studied, only the results of AEI instruments are represented in this study. Different styles of instruments used in this study are presented in Table 1. The instruments were made of 440A high chromium stainless steel. In each coating run, highly polished (R_a<30 nm) witness-coupons discs 1 in. diameter × 1/8 in. thick made of 440A steel were also subjected to the coating deposition process along with the dental instruments.

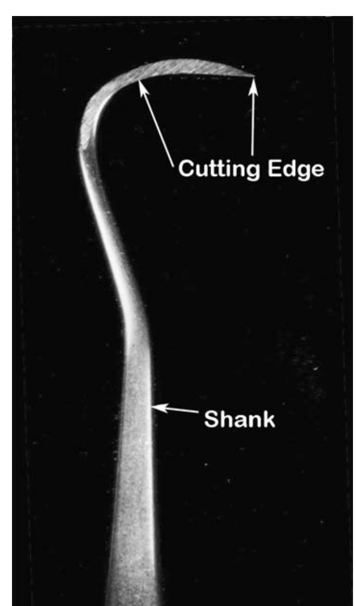

Fig. 1. Photograph of scaling dental instruments.

Table 1
Models of dental instruments used in this study

Item no.	Model number	Model name	Manufacturer	Description
1	G11-12-DP	Gracey Scaler	AEI	Has a longer terminal shank for scaling deep pockets
2	G11-12-DP-L	Gracey Scaler	AEI	Has a longer terminal shank and longer blade
3	G11-57-00	Gracey Scaler	AEI	Short blade
4	G11-57-00-L	Gracey Scaler	AEI	
5	G11-57-30	Gracey Scaler	AEI	

2.2. Deposition of coatings

The multi-layered cermet coatings were deposited on different dental instruments using a large-area filtered arc deposition (LAFAD) system at AEI. This system consists of a cylindrical vacuum processing chamber, 0.5 m in diameter and 0.5 m in height. Inside the chamber, a rotating, carousel-type, 400-mm-diameter substrate platform is installed, having 12 satellite substrate holders capable of planetary rotation about their vertical axes. The substrate platform and its satellite holders provide double rotation, as illustrated schematically in Fig. 2.

The system is capable of holding up to 1400 hand instruments, (scalers, curette tips, composite tool tips, etc.) per run. The dual-arc LAFAD plasma source is attached to the front door of the vacuum chamber. It consists of a rectangular plasma-guide chamber with two rectangular magnetic field coils installed on opposite sides of the chamber. Two cathodic arc sources with rectangular or circular targets are installed on the side-walls of the rectangular plasma-guide chamber and are surrounded by rectangular focusing and deflecting coils. A quasi-flat deflecting magnetic field configuration significantly reduces plasma losses in the direction perpendicular to the plasma-guide walls, while the arc plasma can propagate freely along magnetic field lines to reach remote parts of the deposition chamber. This produces a dramatic increase of output arc current, which can exceed 6 A at a combined input current of 300 A for both incorporated primary cathodic arc sources. Under these current parameters, ionization rate of gaseous

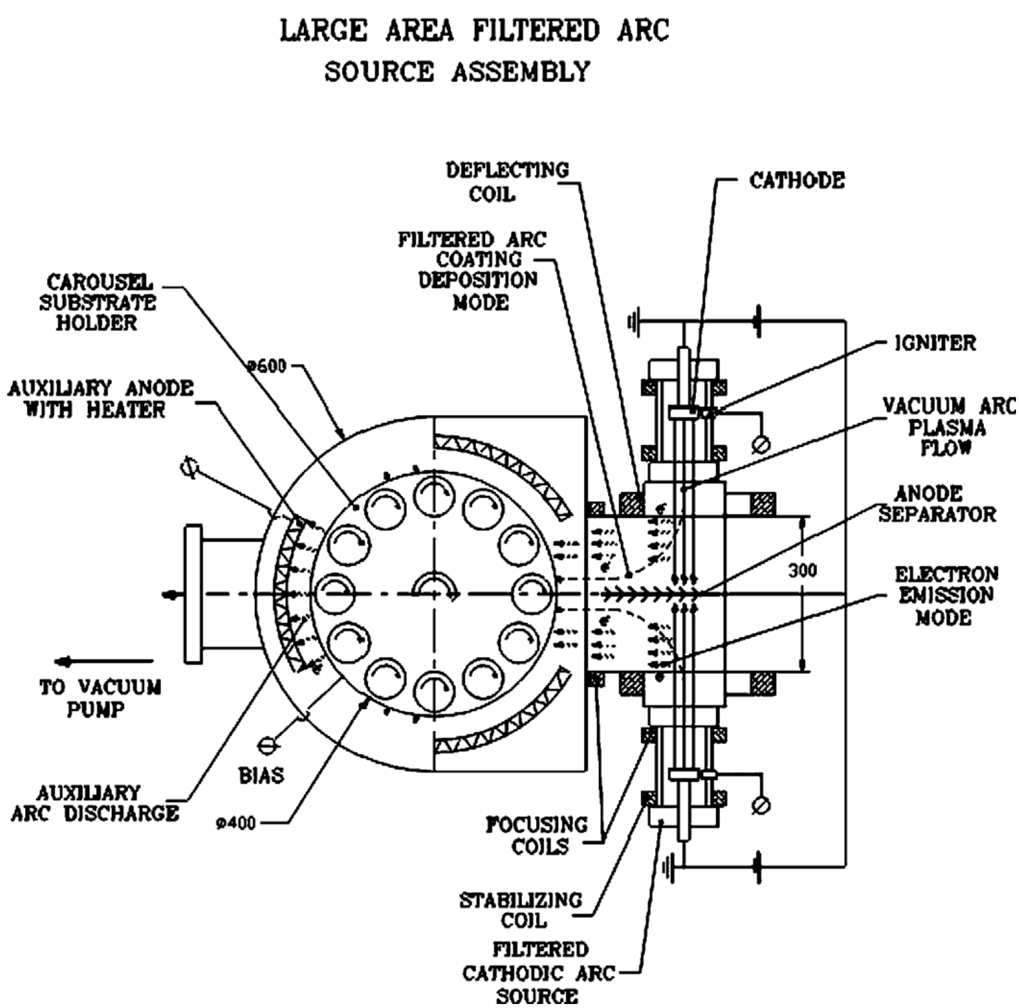

Fig. 2. Schematic view of LAFAD surface engineering system.

plasma component exceeds 30%. This translates into a coating deposition rate of up to 1 μm/h for TiN and related coatings for a fully loaded chamber. Due to the double rotation of the substrate holders, the variation of coating thickness does not exceed ±20%, when using cylindrical, 3-in.-diameter, titanium targets of primary cathodic arc sources. The uniformity of coating thickness can be improved, by adding vertical magnetic rastering, to better than ±10%, and further improved to as low as ±2%, by using rectangular cathode targets. The vacuum arc cathode is also a theoretically unlimited electron emitter, thereby providing an efficient source of high-density electron current. In this mode, it facilitates the generation of a uniform, high-density plasma cloud in the processing chamber. This produces a "plasma-immersed" environment, which provides a uniform condition for plasma ion etching, ion nitriding, low-energy ion implantation and plasma-assisted chemical vapor deposition. The detailed description of LAFAD technology can be found elsewhere [4–6].

The typical LAFAD process for deposition TiN/Ti multilayer coatings consisted of heating and outgasing the substrates, sputter cleaning, metal ion etching, deposition of a metal bond layer, followed by the deposition of the multilayer coating, consisting of the following steps:

1. Substrate dental instruments were ultrasonically washed and dried in an oven at 150 °C.
2. The instruments were loaded into the coating chamber under clean, dust-free conditions.
3. The chamber was evacuated to ultimate vacuum of about 6×10^{-4} Pa.
4. The substrates were heated by means of radiant heating to 400 °C. The heating stage lasted for 1 h.
5. The substrates were ion cleaned in argon at 10^{-1} Pa for 20 min. During ion cleaning stage, the bias voltage was set up at 250 V,
6. The substrates were then Ti metal ion etched for 2 min, at 1000 V at argon pressure of 2×10^{-2} Pa.
7. The initial metal bond layer was deposited at a working pressure of 4×10^{-2} Pa and a substrate bias of -200 V (RF).
8. Multilayer Ti/TiN coating was deposited by switching the atmosphere from argon to nitrogen mixture. Typical working pressure, substrate bias, and substrate temperature for the coating deposition stage were 4×10^{-2} Pa, -40 V, and 350–400 °C respectively.

The coating composition, used in most cases that are reported in this work, was TiN/Ti multilayer coating. In some cases, coatings of TiZrN/TiZr composition with architecture similar to the TiN/Ti multilayer were also used. The architecture of these coatings is shown schematically in Fig. 3A [18].

Using targets made of different metals on opposite sides of LAFAD plasma source (Fig. 2) created more complex nanostructured coating architectures. One example of such processes is presented by TiCrCN gradient multilayer superlattice coating. This coating consists of two segments: the bottom segment, utilizing TiCrN/TiCr multilayer superlattice nitride coating, and the upper segment, utilizing TiCrCN/TiCr multilayer superlattice carbonitride coating. This can be noted as [TiCrN/TiCr]–[TiCrCN/TiCr] coating architecture. The ceramic/metal bi-layer period in each of these two segments ranges from 300 to 400 nm, while the bi-layer period in a superlattice ranges from 2 to 3 nm and can be controlled by rotation speed of carousel substrate platform. The intermediate gradient layer is created between the nitride and carbonitride coating segments by increasing the concentration of ethane in nitrogen/ethane reactive gas atmosphere. The architecture of the bottom segment of this coating (TiCrN/TiCr) is shown schematically in Fig. 3B.

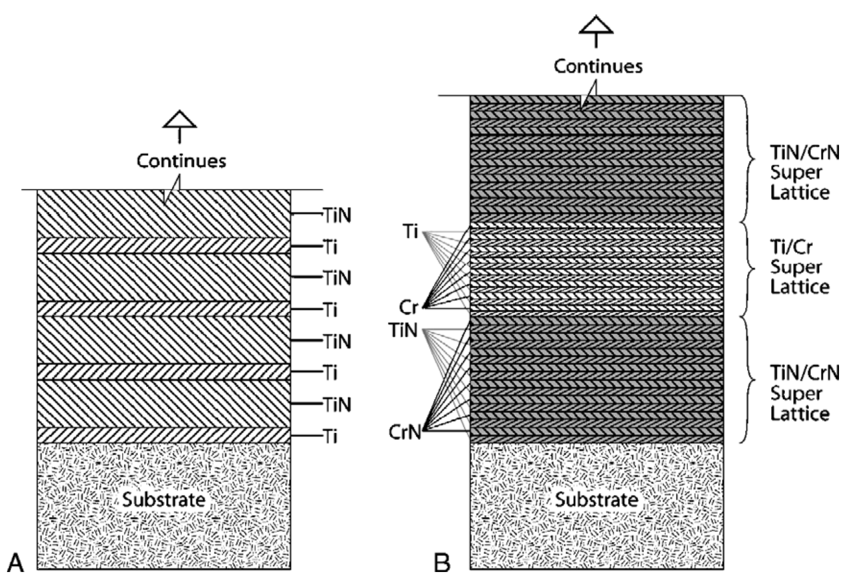

Fig. 3. Schematic illustration of coating architecture: (A) TiN/Ti multilayer; (B) TiCrN/TiCr superlattice multilayer coating.

Several coatings were prepared using duplex technology. In this process, the steel substrate is first subjected to ionitriding in pure nitrogen plasma immersion environment created by LAFAD plasma source in auxiliary arc discharge mode [4,5]. In this mode, the deflecting magnetic subsystem is not activated and LAFAD source is working as a powerful electron emitter in a pressure ranging from 0.05 to 0.1 Pa. This stage is followed by deposition of TiN/Ti multilayer coating by the process outlined above.

2.3. Characterization and testing

Coated dental instruments and coating properties were characterized by variety of techniques. The following methods were used to determine the film's properties:

(1) The coating thickness was measured by the ball wear scar (Calotest™) technique.
(2) The test method specified by Daimler Benz was used in determining adhesion. Its classification scheme is shown in [10].
Both (1) and (2) methods were applied to coated witness-coupons, since they require flat well-polished surfaces.
The following method was used for evaluation of adhesion on coated round-shape dental instruments of different grades:
(3) The shank of the selected dental instrument was sheared by standard ductility test device at different locations and the coating delamination around the shared area was examined by optical microscopy. This test was also used for the measurement of ductility of the steel shanks.
(4) Scanning electron microscopy (SEM) and reflective optical microscopy were used to examine morphology of films and instrument surfaces. The backscattering electron imaging (BEI) technique, displaying surface composition, was found beneficial for examining wear lands on coated instruments.
(5) Surface profile was evaluated by atomic force microscopy (AFM).
(6) Film composition was measured by energy dispersion spectroscopy (EDS).

2.4. Testing for instrument durability, wear and cutting performance

Three stroke testing devices were used for laboratory simulation of the scaler–tooth interaction. In spite of certain differences in design, all of the devices had a means to provide a linear back-and-forth movement of test scalers against tooth or simulated tooth material. An adjustable weight was attached to the scaler holding arm to allow control of the load on the cutting edge of the instrument to better simulate the intra-oral working conditions. A small water pump was used to provide constant water flow over the scaler and the tooth to provide constant hydration of the tooth material to remove scraped substrate debris and to better simulate moist intraoral environment. This device is shown schematically in Fig. 4.

A custom mechanical stroke device from the Biomaterials Division in Dentistry of the University of Toronto (UofT) was extensively modified to include features capable of simulating the load and motion of dental scalers against enamel and dentin tooth surfaces in an aqueous environment. This device has the ability to test six scalers simultaneously. At UofT, tests were conducted in normal saline with the working blades of instruments sliding against the enamel of bovine teeth. The contact load between the cutting edge of the scaler and the enamel surface was 120 g and the travel length was 20 mm per scaler cycle. The instrument blade was lowered onto the enamel at the beginning of each pull stroke and raised off the enamel at the end of the stroke. A bi-directional pneumatic cylinder

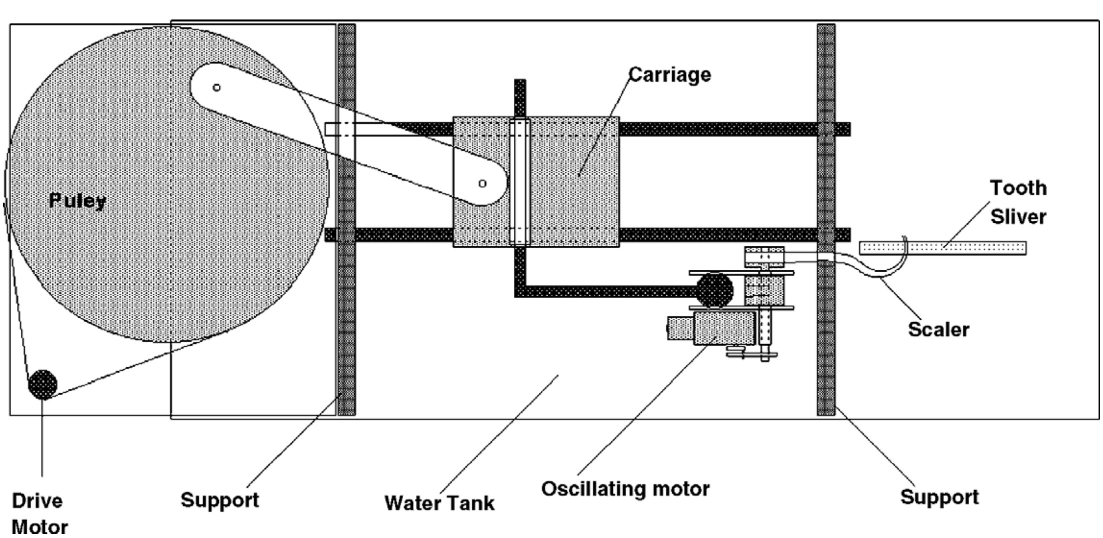

Fig. 4. Schematic view of stroke testing apparatus.

controlled the raising and lowering motion. The air pressure, used to operate a pneumatic cylinder, controlled the timing and rate at which the instrument was lowered onto the enamel. This control minimized the potential detrimental effects of impact loading on the cutting edge and fatigue fracture of the cutting blade.

The stroke testing apparatus at AEI used a bi-directional motion of the scaler, with the stroke length of 15 mm and the pressure of 150 g. The motion was produced by a bi-directional pneumatic cylinder.

The apparatus used by Dr. Bekesch used a bi-directional stroke of 25 mm at a pressure of 100 g. The motion was produced by a cam operated by an electric motor. This apparatus also had an additional electrically operated cam on the scaler holding arm to provide additional oscillation of the scaler to better simulate the varying angle of attack the scaler makes with the tooth in vivo.

At UofT, SEM micrographs of the cutting edges were made at magnifications of 100 and 1000 after 0, 500, 2000 and 5000 cycles of sliding contact against bovine enamel. The 100× magnification micrographs were used to construct a composite graphic along the length of the cutting edge of the blade to assess whether wear was uniform over the length of the blade. Wear was determined by measuring the width of the cutting edge of the instruments at four stages: (1) as received from AEI and (2) after 500, 2000 and 5000 cycles. Instruments were coded so that any differences in coating variables between coated instruments were unknown during the evaluation process.

Two additional methods were used to evaluate wear of cutting edge. One used optical microscopy. In this case, the wear area was examined under different magnification. It used light microcopy to make a subjective evaluation of cutting edges of new instruments and coated instruments with different thickness of multi-layer coatings. In this assessment, the magnification required to see the first clear signs of wear was recorded for various numbers of cycles from 0 up to 15,000.

In another evaluation, the photomicrographs of cross sections of the working heads were used in order to assess wear of coated and non-coated instruments at various numbers of cycles.

For practical purposes, the instrument was considered blunt when the observable cutting edge exceeded 30 μm.

2.5. Testing for corrosion resistance to ultrasonic cleaning and steam sterilization

Ultrasonic cleaning followed by steam sterilization is the most effective method of instrument sterilization in the dental office. Five new non-coated and five new coated instruments were subjected to 215 cycles of ultrasonic cleaning followed by steam sterilization in a Castle steam sterilizer. In addition, the new working blade of coated instrument C12-27 was included in the coated group. This blade was used to evaluate the effects of sterilization on wear. Ultrasonic cleaning was performed using a 10-min time period in a general purpose aqueous cleaner (IMS Daily Clean) in a 90-W L&R T-14B ultrasonic cleaner. For sterilization, both the control and test instruments were placed in instrument cassettes and were included in the normal sterilization cycles used to sterilize conventional office instruments. Each cycle consisted of 30 min at 260 °F with a 20-min drying time. The blades of the test instruments and respective controls were inspected visually and with 40× binocular microscopy after 50, 100, 150 and 215 sterilization cycles. There was no evidence of tarnish or pitting corrosion on either the control (non-coated) or coated instruments at the evaluation intervals. In an accelerated version of this test routinely used as a QC test in AEI, the articles are enclosed in plastic enclosures and placed in an autoclave at 15 PSI (1 atm above ambient) pressure and 134 °C for 50 min.

3. Results and discussion

3.1. Coating properties

The difference between TiN coatings deposited by conventional direct cathodic arc deposition (DCAD) technology and LAFAD process is illustrated in Fig. 5.

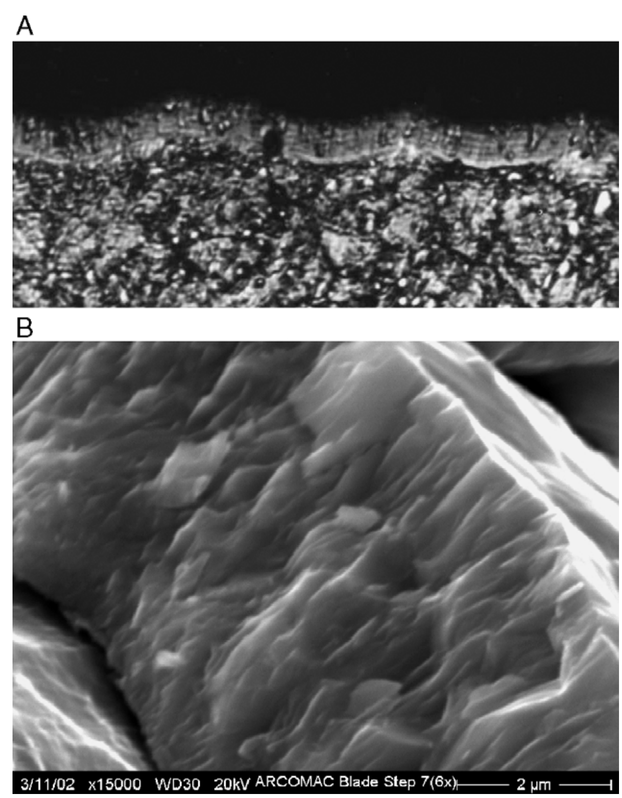

Fig. 5. Morphology of TiN single-layer coatings deposited by cathodic arc deposition PVD technology: (A) micro-droplets incorporating in vacuum cathodic arc deposition TiN coating; (B) fracture of filtered arc TiN coating.

A photomicrograph of a metallurgical cross section of a steel substrate S and the DCAD titanium nitride single-layer coating, with thickness about 5 μm, is shown in Fig. 5A. It consists of macroparticles of α-Ti, D incorporated in the deposited TiN matrix C. This contrasts with the columnar, polycrystalline TiN single layer, without any inclusions or voids, which is deposited by LAFAD process as shown in Fig. 5B. Eliminating macroparticles and growth defects is critically important for achieving high performance of corrosion-resistive coatings. It has been found that corrosion resistance of 440 steel varies with the quality of the surface finish. When the substrate surface was highly polished, the pitting corrosion starts on macroparticles and growth defects at the coating to substrate interface [5,8,11,12]. The rate of deposition can be estimated by measurement of the coating thickness of TiN/Ti multilayer coating deposited by a 5-h LAFAD coating deposition run. This measurement, based on the wear scar technique (CALOtest), was prepared on stainless steel "witness" disk coupons. This measurement shows 2.7 μm coating thickness for double rotation, and 5.3 μm for single rotation, resulting in 0.54 μm/h and 1.06 μm/h deposition rate for double and single rotation, respectively. These deposition rates are in agreement with previous measurements [4]. The actual coating thickness on dental instruments can differ from that of flat coupon. It can be estimated based on wear scar area of scaler subjected to stroke test.

An optical photomicrograph of a cross section of a Gracey curette, ionitrided in LAFAD plasma immersion process is shown in Fig. 6. The rate of ionitriding in auxiliary arc plasma ranges from 0.5 to 1 μm/min for 440A stainless steel [4]. The microhardness measured on the surface of ionitrided 440A steel by Knoop microhardness indentation with 0.5-N load ranges from 1.1 to 1.3 GPa.

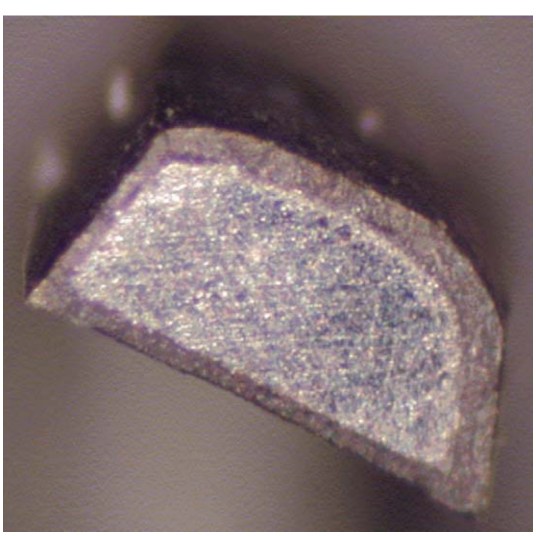

Fig. 6. Cross section of curette subjected to duplex surface treatment by LAFAD process: ionitriding following by TiN/Ti multilayer coating.

Table 2
Coating elemental composition

Sample number	Ti (at.%)	Zr (at.%)	Cr (at.%)	C (at.%)	N (at.%)
TiN28-1	59.04	–	–	Not shown	40.76
TiN28-2	59.26	–	–	Not shown	40.74
TiN28-3	60.38	–	–	Not shown	39.39
TiZrN12-1	33.43	14.65	–	Not shown	51.92
TiZrN12-2	37.36	16.71	–	Not shown	45.93
TiZrN12-3	39.10	17.69	–	Not shown	43.21
TiZrN12-4	36.77	16.04	–	Not shown	47.19
TiCrCN (top)	31.34	–	14.32	27.66	26.68

The micro-hardness of a single-layer TiN coating deposited by direct (unfiltered) cathodic arc ranges from 20 to 25 GPa while the micro-hardness of a LAFAD TiN coating can range from 30 to 35 GPa [4–9]. The negative consequences of super-hard properties of thick, filtered arc coatings are their brittleness and internal stresses. The multi-layer coating architecture can enhance the flexibility of the coating and to eliminate brittle fractures [5,8,12,16,17]. It consists of a number of alternating metal–ceramic bi-layers as shown in Fig. 3. The thickness of the metallic interlayer typically ranges between 50 and 100 nm, while the thickness of the ceramic interlayer ranges between 300 and 500 nm. The metallic interlayer reduces the internal stresses and serves as a spring suspension between neighboring hard cermet sublayers. It provides significant flexibility of the entire coating structure. Typical elemental composition of TiN/Ti, TiZrN/TiZr and TiCrCN coatings deposited by LAFAD process are presented in Table 2. The EDS spectra taken from several spots of two samples show near-stoichiometric coating composition.

Fig. 7 outlines the change in surface profile after depositing thick TiN/Ti coating by LAFAD process. Fig. 7A shows the AFM image of uncoated metallographically polished stainless steel coupon having initial roughness $R_a \lesssim 2$ nm. Fig. 7B shows the AFM image of the same coupon coated by a 7.5-μm TiN/Ti coating. It can be seen that the average roughness gains less than 10 nm at total thickness increase of 7.5 μm despite the columnar morphology of this multilayer TiN/Ti coating. This can be attributed to high surface mobility of deposited adatoms due to their kinetic energy which exceeds 40 eV for Ti ions generated by vacuum cathodic arc process [7].

The SEM image of the typical HRc indentation of 3-μm-thick TiN/Ti coating is shown in Fig. 8. The radial cracks with no delaminations outline excellent coating adhesion. The SEM image of a sheared scaler shank with TiN multilayer coating, with thickness of about 3 μm, is shown in Fig. 9. It shows the cracks developed through the coatings as a result of large plastic deformation of the substrate. But at the same time, it shows no delaminations up to the edge of the sheared area, demonstrating super-adhesion properties of LAFAD cermet coatings. It has to be noted that similar coatings, deposited without the high-

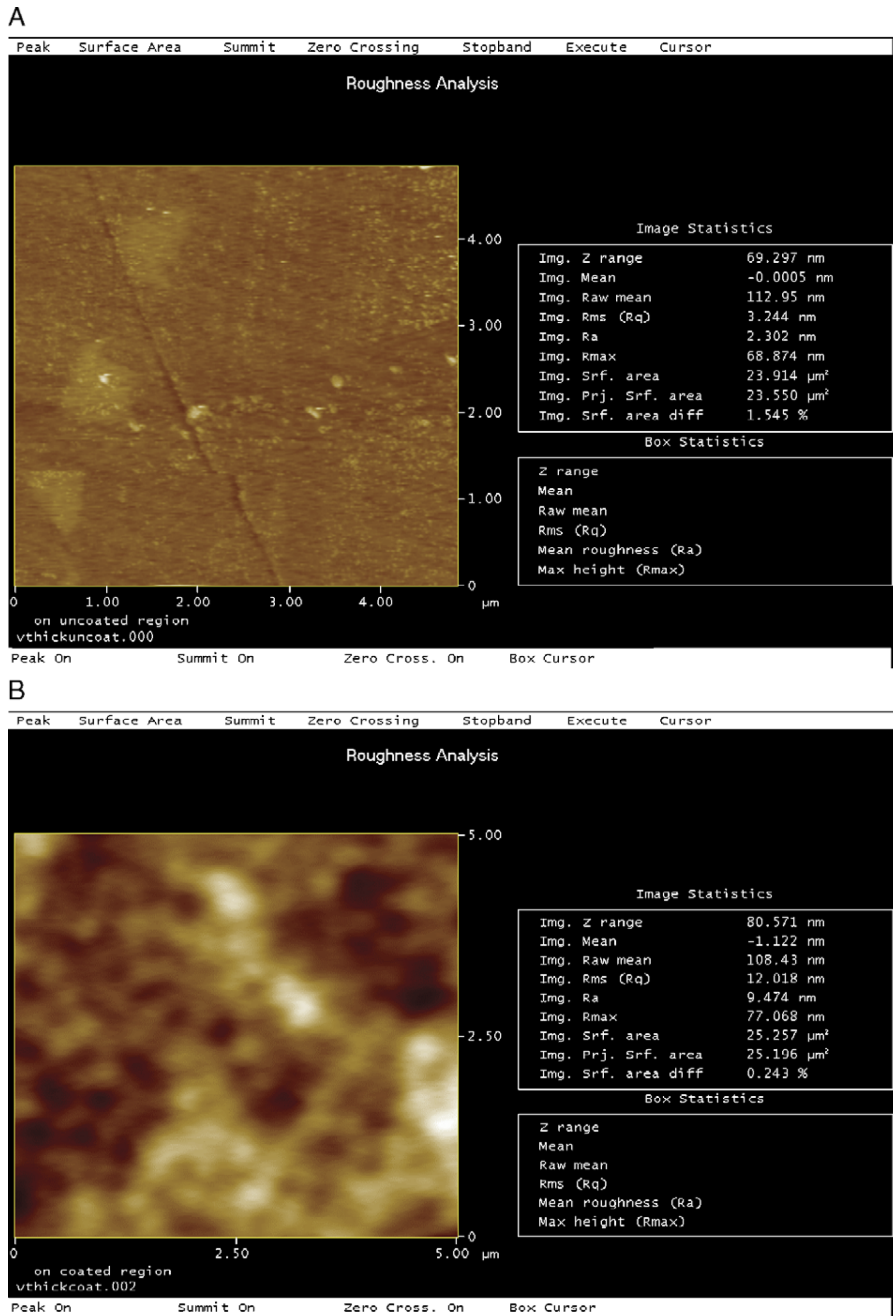

Fig. 7. AFM image and roughness parameters of TiN/Ti coating deposited on metallographically polished stainless steel coupon: (A) uncoated coupon; (B) coupon coated by 7.5-µm-thick TiN/Ti coating.

voltage metal ion etching step, display catastrophic delamination around the edge of the sheared area.

The abrasion wear resistance of the TiN/Ti multilayer coatings was examined by subjecting the coated dental instruments (endodontic files) to vibratory tumbling in a vat, containing a cellulose filler and an abrasive. The quartz sand with characteristic particle size of about 500 µm was used as the abrasive. Fig. 10 shows the surface of the instruments with and without TiN coating after exposure to vibratory tumbling for 24 h. It can be seen that sharpening striations are almost completely polished off on the uncoated instrument surface (Fig. 10A), while they remain untouched on the coated instrument (Fig. 10B).

3.2. Instrument performance in laboratory tests

Fig. 11, showing reversed magnification vs. number of scaler strokes, indicates that instruments with four layers of TiN/Ti multilayer coating require approximately eight times more cycles (8000) to produce the same amount of wear that

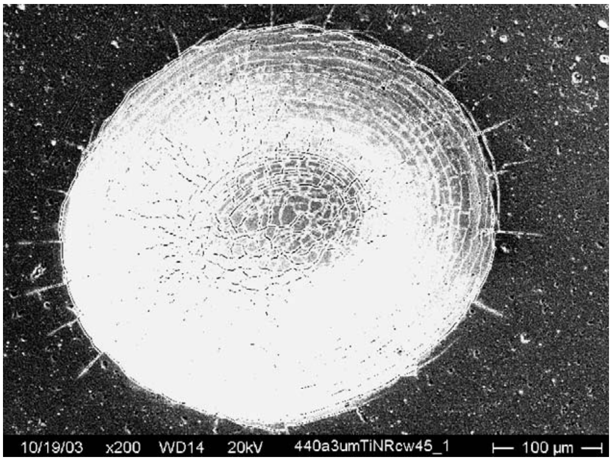

Fig. 8. SEM image of HRc indentation of 3 μm TiN/Ti multilayer coating deposited on 440a stainless steel.

is seen on non-coated instruments at 1000 cycles. The same figure indicates that instruments with 10 coats of TiN/Ti require approximately 12.5 times more cycles (12,500) to produce the same amount of wear that is seen on non-coated instruments at 1000 cycles. When the nitride coating is penetrated, the rate of wear rapidly approaches that of non-coated blade.

The bar chart (Fig. 12) shows widths of the cutting edge for each instrument in micrometers measured from SEM photomicrographs made at a magnification of 1000×. The instrument codes are shown on the horizontal axis. The first seven instruments were coated. The last four instruments were not coated. All the coated instruments showed an increase in the width of the cutting edge from approximately 1 μm before testing to an average of 3.4 μm after 5000 cycles. The control (non-coated) instruments showed an increase in the width of the working edge from approximately 1 μm, before testing, to an average of 35 μm after 5000 cycles. The non-coated blades showed 10.3 times more wear than the coated ones.

The cutting edge of C12-27 that was subjected to 215 sterilization cycles was measured and tested at 500, 2000 and 5000 stroking cycles. These repeated ultrasonic cleanings and sterilization in corrosive chemicals under elevated temperatures had no effect on the wear rate of the instrument. SEM examination of the instrument surface showed no evidence of pitting or any other alteration of the coating due to the sterilization and cleaning cycles.

Fig. 13 shows the results of using photomicrographs of the cutting edge cross sections in order to assess wear of coated and non-coated instruments at various numbers of cycles. Comparison of the photomicrographs of the cross sections of instruments at a representative point on the blade indicates that the wear of non-coated instruments after 1000 cycles (Fig. 13A) is roughly similar to the wear of coated instruments at 10,000 cycles (Fig. 13B).

The methodical assessment of the degradation of cutting edges of Gracey curettes during stroke test is presented in Fig. 14. It shows the increase of the wear land of coated and uncoated instruments vs. number of strokes. In agreement with previous observations, it can be seen that coated instruments have edge degradation rate 10 times less than uncoated instrument. The Fig. 15 shows the SEM images of uncoated instrument after 1200 strokes vs. coated instruments after 12,000 strokes. Both instruments were taken from the batches used in chart shown in Fig. 14. The difference in wear land widths is approximately 10 times.

The wear land of uncoated instrument in stroke test progresses almost entirely by abrasive wear. This abrasive blunting progresses linearly until the wear land is so broad that the instrument becomes unserviceable. The coated instruments wear in a different way. They appear to wear in two phases. Initially, the wear is by a very slow abrasive polishing of the coating, leading to a polished wear land on the main cutting edge. This process takes place over many thousands of strokes. Fig. 16A shows this polished wear land after 4000 strokes against bovine dentine in a laboratory stroking device. Because this is purely abrasive wear in a low wear configuration, once this polished wear land is established, successive wear progresses even slower due to the decreasing specific load on the cutting edge as the wear land expands. This stable situation can be observed up to about 10,000 strokes as shown in Fig. 16B. It can be seen that when the number of strokes increases, the polished coating area around cutting edge increases followed by expansion of the wear land. Eventually, the cermet coating wears through and the underlying metal also begins to wear.

The microimages of the cutting edges of the scalers subjected to 12,000 strokes are shown in Fig. 17. Fig. 17A shows BEI compositional image of the cutting edge of the scaler, with TiN/Ti multilayer coating. The wear land contains approximately even widths of exposed metal and

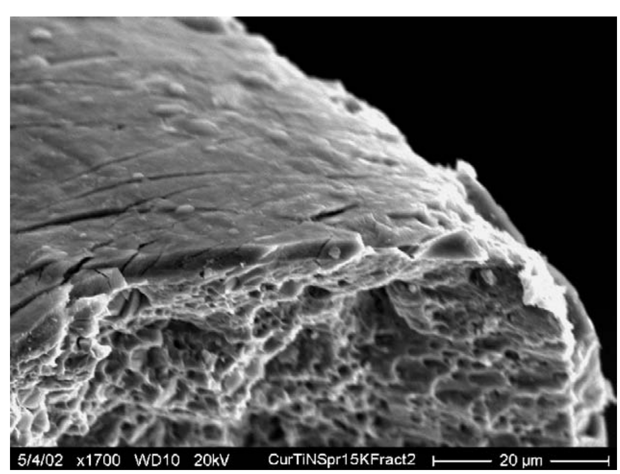

Fig. 9. SEM image of sheared scaler shank. Scaler has 3 μm TiN/Ti multilayer coating.

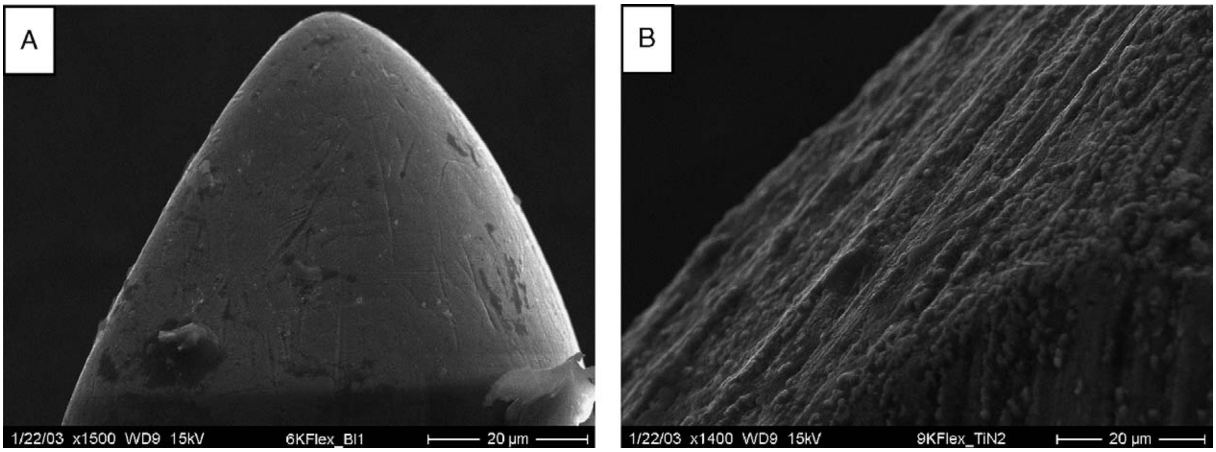

Fig. 10. Surface of the tips of endodontic files made of stainless steel, subjected to 24 h of vibratory tumbling: (A) uncoated instrument; (B) TiN/Ti multilayer coated instrument.

the polished coating. Undamaged coating covers the rest of the instrument. It demonstrates the multilayer coating architecture. The coating is being exposed layer by layer in a rub-through process. One can see the exposed steel substrate S, and the layered coating C with a laterally propagating crack between superficial sublayers. This lateral propagation of the crack is due to the multilayered architecture of the coating. Thin superficial layers of the coating may be lost but the underlying sublayers remain to provide continued protection. This is radically different from the behavior of a single-layered thick coating. There the cracks would propagate perpendicularly to the surface, producing crumbling of the coating and early exposure of the metal substrate.

Fig. 17B shows SEM image of the cutting edge of the scaler having TiZrN/TiZr multilayer coating after a stroke test. It can be seen that the coating surface is replicating the substrate's surface profile including the sharpening striations. The entire wear land can be broken down into three sections: the wear scar of the coating on the sharpened side of the blade, the exposed substrate metal, and the wear scar of the coating on the face (unsharpened) side of the blade. The average sizes of each of these areas can be found from Fig. 17B. The schematic illustration of the cross section of this instrument is shown in Fig. 18. In this case, the l_s, l and l_f are representing thicknesses of the wear scar area on sharpened side of the blade, the width of exposed substrate metal area and the wear scar of coating on face side of the blade, respectively. Based on this model, and assuming that the coating thickness is equal on both sides of the blade, the following expression can determine the relationship between l_f/l_s ratio and the angle (β) of declination of the

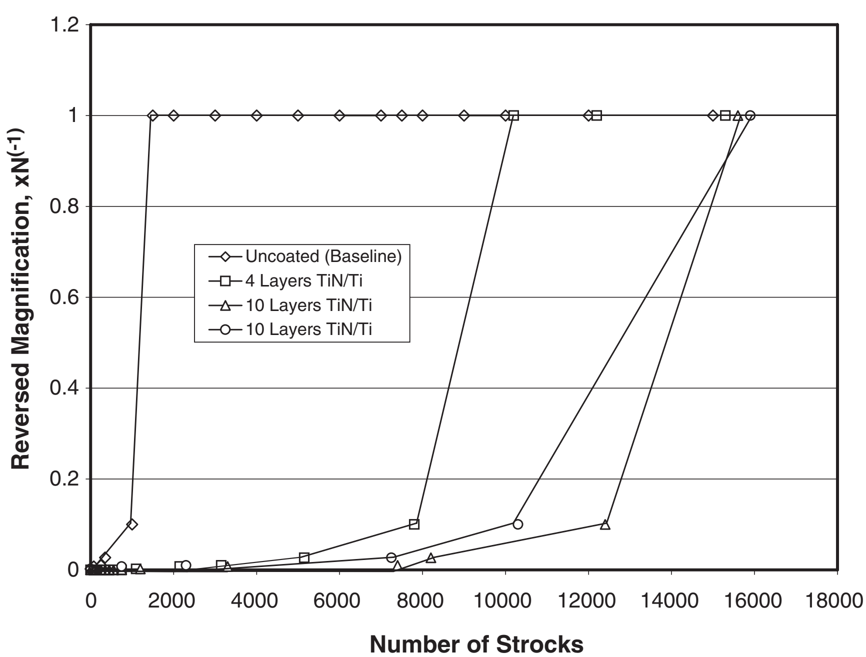

Fig. 11. Optical assessment of wear on the edges of scalers.

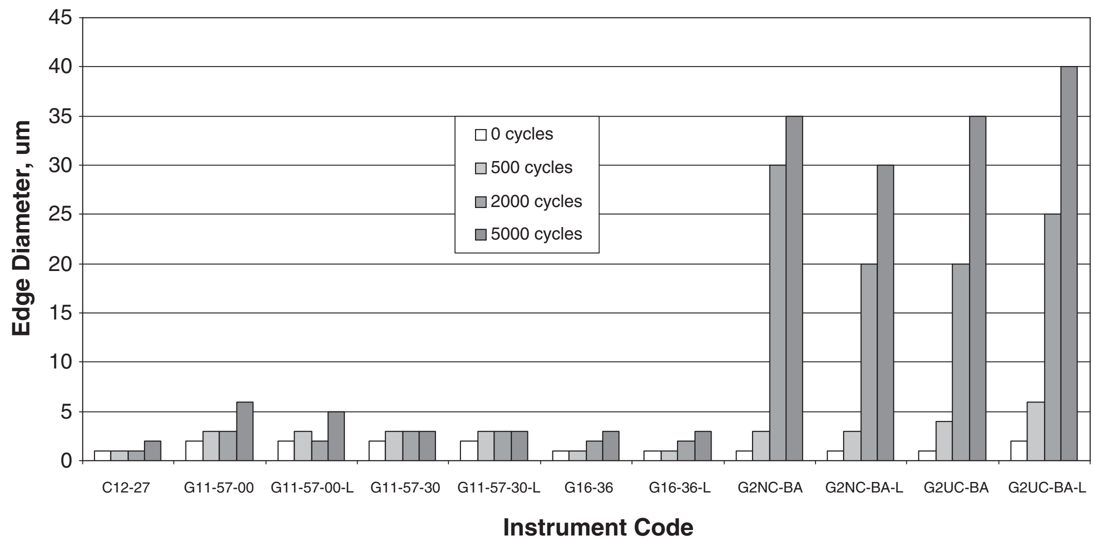

Fig. 12. Chart representing wear of different instruments obtained by stroke testing at the University of Toronto Faculty of Dentistry.

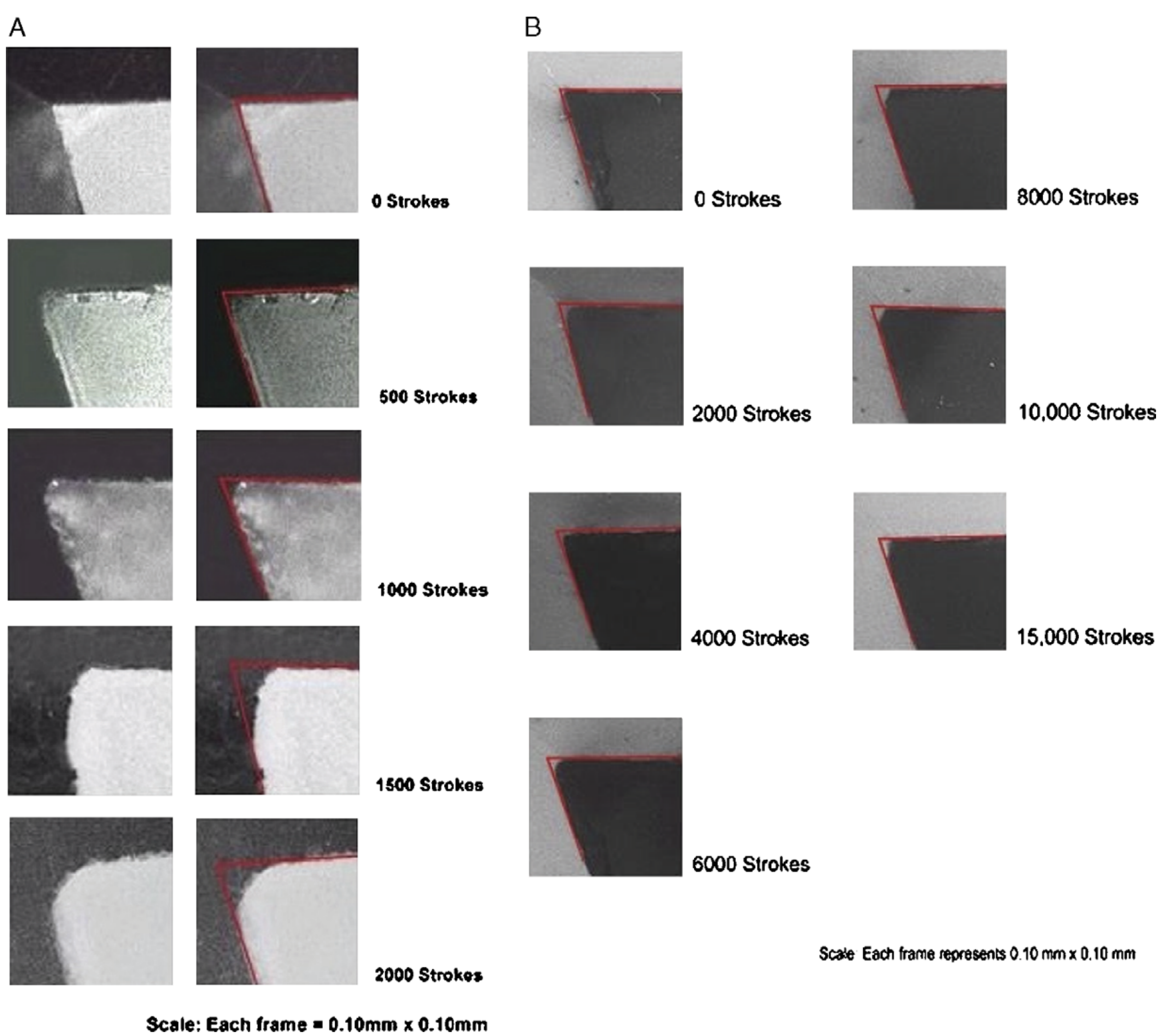

Fig. 13. Micro-cross sections of scalers subjected to stroke test: (A) cross section with reference profile of uncoated scalers (baseline); (B) cross section with reference profile of scalers with 10 TiN/Ti bi-layers. Notice: Images are of different scalers due to the process of imaging each stage.

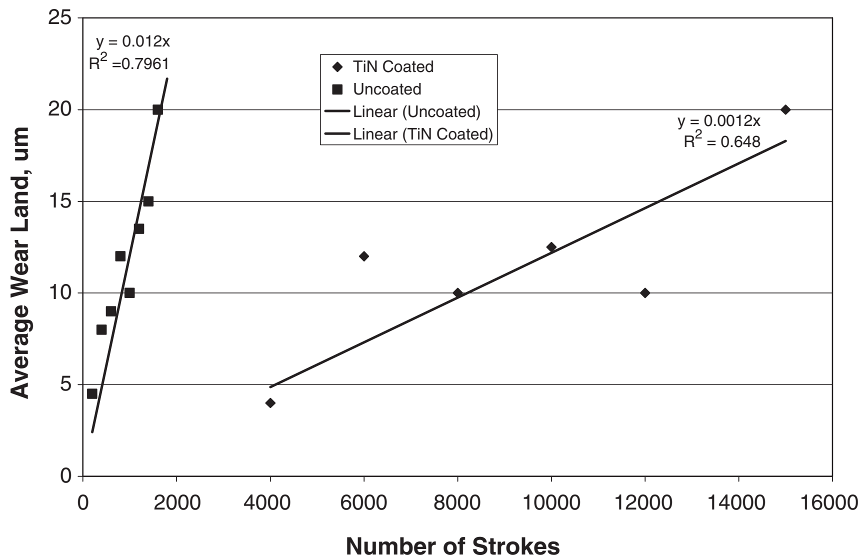

Fig. 14. Wear rate of coated vs. uncoated instruments in stroke test.

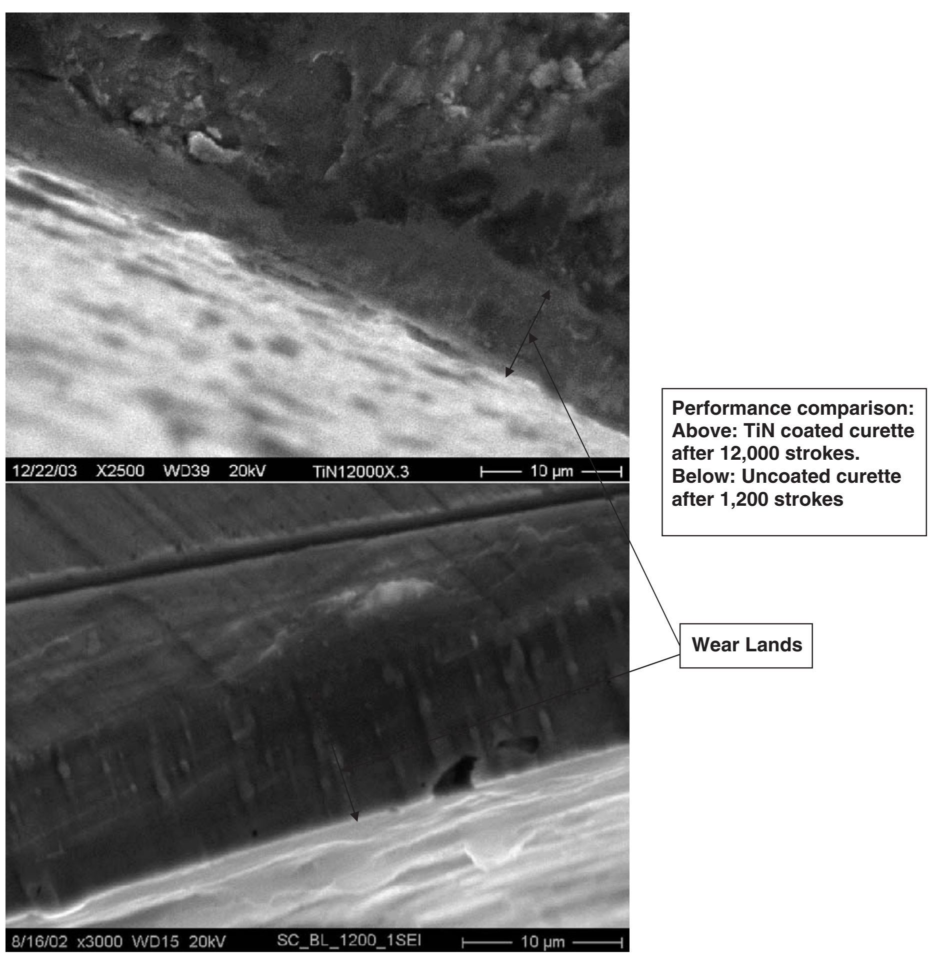

Fig. 15. SEM view of cutting edges of coated scaler at 12,000 strokes and uncoated scaler at 1200 strokes.

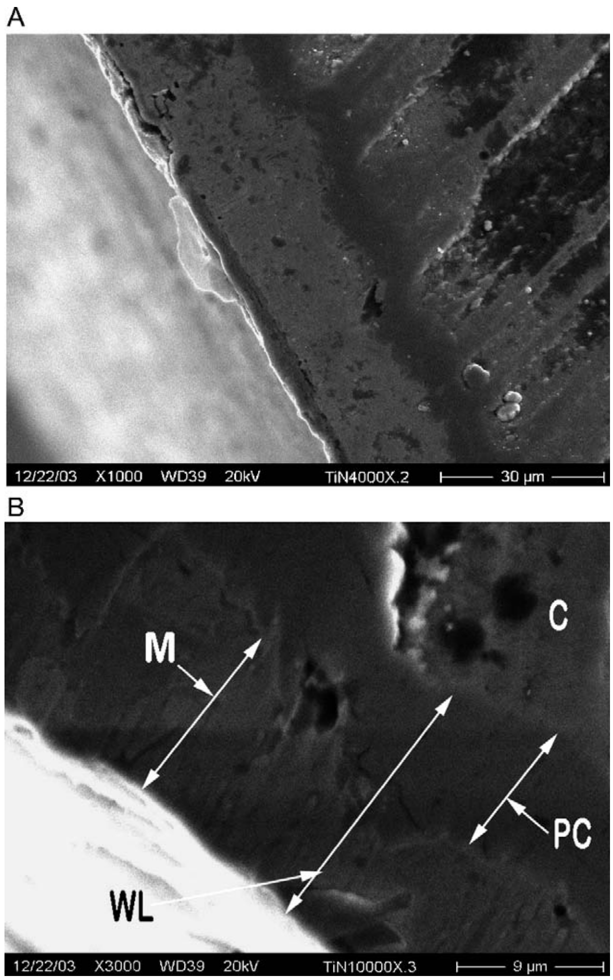

Fig. 16. SEM view of the cutting edge of scalers after 4000 strokes (A) and after 10,000 strokes (B).

wear scar area to the plane of the sharpened side of the blade:

$$l_f/l_s = \cos\gamma + \sin\gamma ctg\beta \tag{1}$$

This allows to estimate the coating thickness near the cutting edge of the instrument: $d = l_f \sin\beta$. For example, the coating thickness determined by this procedure, using parameters taken from Fig. 19B, will be $d = 1.9$ µm, which is in agreement with CALOtest measurements. The wear rate of the cutting edge in this stroke test can then be determined by the following expression:

$$\dot{M} = \dot{m}_c l_s + \dot{m}_{St} l + \dot{m}_c l_f, \tag{2}$$

where $\dot{m}_c$ and $\dot{m}_{St}$ are wear rates of coating and stainless steel, respectively. Taking into account that $\dot{m}_c << \dot{m}_{St}$ and $l_f/l_s << 1$, one can estimate the abrasion wear rate of the cutting edge as

$$\dot{M} \approx \dot{m}_c l_s \tag{3}$$

This estimation can be used at least until the width l of the substrate steel exposure does not significantly exceed the coating wear scar width l_s.

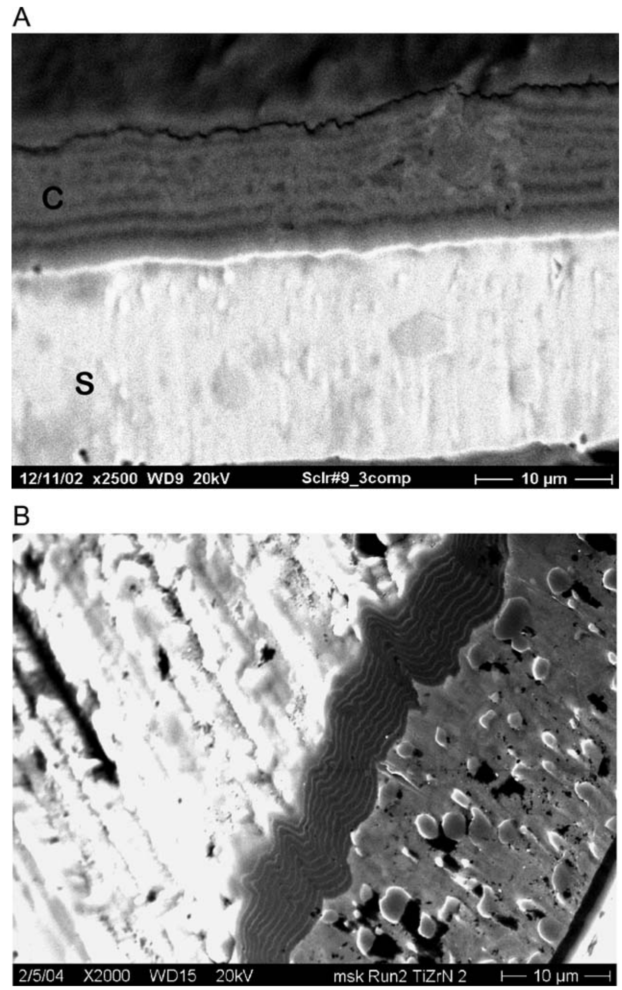

Fig. 17. BEI image of scaler with TiN/Ti multilayer coating 4.5 µm thick after 12,000 strokes (A) and SEM image of scaler with TiZrN/TiZr multilayer coating 2.5 µm thick after 9000 strokes (B).

Further improvement of abrasion wear resistance can be achieved by using more complex coating architectures [5,8,17]. Fig. 19A shows the BEI image of cutting edge

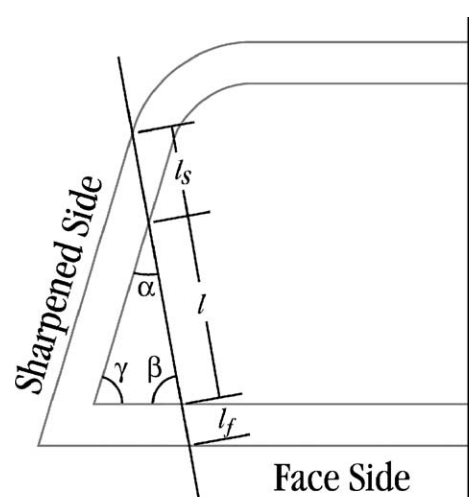

Fig. 18. Schematic representation of scaler wear land in stroke test.

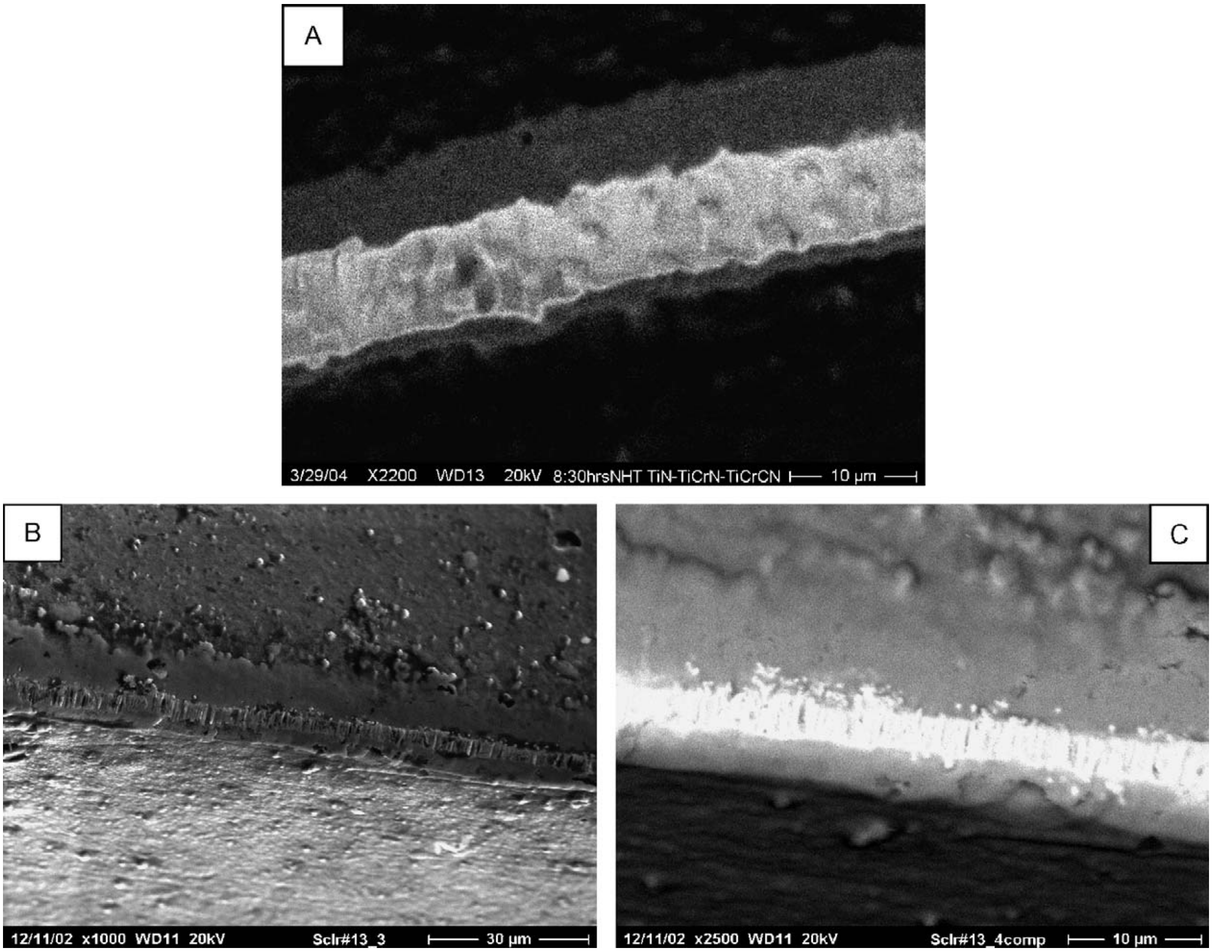

Fig. 19. Cutting edge of scaler having multilayer superlattice TiCrCN coating and duplex surface treatment (ionitriding followed by TiN/Ti multilayer coating) after 9000 strokes: (A) TiCrCN BEI image; (B) iN+TiN/TiN SEM image; (C) iN+TiN/TiN BEI image.

of scaler having [TiCrN/TiN]–[TiCrCN/TiCr] gradient multilayer superlattice coating. The exposed area of the cutting edge after 9000 strokes does not exceed 8 μm. Elemental chromium containing in the metallic TiCr interlayers also contributes to significant increase in corrosion resistance by forming a chemically stable chromium oxide in corrosion environment. Fig. 19B and C shows the cutting edge of scaler subjected to duplex surface treatment: ionitriding followed by multilayer TiN/Ti coating after 9000 strokes. It can be seen that the wear scar area is just started to develop. One can estimate that this duplex technology should yield an additional 50% improvement in wear resistance over the simple TiN/Ti multilayer coating. Both these tests were prepared with 150 g load.

Since the results from four independent studies all show roughly a 10-fold increase in wear resistance with LAFAD multi-layer coatings, there is no doubt that there is a large increase in wear resistance with coated instruments. Such an improvement will make an important difference to dentists using these instruments. It appears that 10 multilayers (TiN/Ti) are optimal. The coating acts as a protective shield. It wears very slowly due to the high hardness differential between the coating and the tooth material. This protective function of the coating prevents the wear of the metal until the coating wears through. Once the protective coating is penetrated the wear pattern begins to approach that of the uncoated instrument. In this case, the wear rate of the instrument is determined by wear rate of coating material since the wear rate of exposed steel

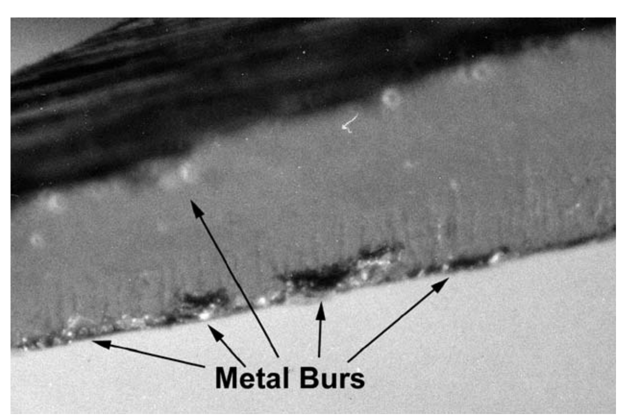

Fig. 20. Optical view of metal burs produced during sharpening.

is more than an order of magnitude greater than that of the coating.

3.3. Instrument performance in clinical tests

Fig. 20 shows an optical photomicrograph of a cutting edge of an uncoated instrument. The edges of the uncoated instrument can be considered as having a microfinish (order of magnitude of the edge radius) on both edges. The last finishing operation was on the flank side, which leaves some thin metal burs hanging over the rake face. These burs are also produced whenever the instrument is resharpened. In vivo, these burs will break off as soon as the instrument is used against a hard surface of the tooth; however, the thin, microscopic pieces of metal can easily imbed into the surrounding soft tissue and can potentially produce inflammatory foreign body reactions in the very delicate gingival margin. Since most of the periodontal scaling is performed by tactile sensing below the gum margin, and since there is usually some bleeding associated with the scaling, such metal fragments would be totally undetectable. These fragments would not be detectable radiographically since their size is below the resolution of standard intraoral radiographs. The inside of the periodontal pocket frequently contains granulation tissue which is usually so loose that any such fragments would penetrate into the granulation tissue and become totally impervious to removal. The marks on the rake faces are certainly caused by the various handling operations following the final honing, since it is indeed very difficult to preserve the finish of such soft polished surfaces.

Coated instruments do not have any burs on the edges due to pre-deposition mechanical treatment operations. The hard coating provides a perfect protection against handling scratches. Wear in the field tests differs from the wear in the laboratory tests in many ways. The differences can be traced to the fact that in practical use, each stroke differs and the wear is the result of each operator's stroke history (or patient sequence).

The main factors that determine the type of wear are:

1. The density and quantity of the calculus attached to the teeth.
2. The presence of overhanging margins of restorations made of hard substances (ceramic, nickel–chromium alloys, gold alloys, amalgam, or composites with different size filler particles made of a variety of materials).
3. The force used by the operator to remove the calculus.
4. The care the operator uses to avoid the margins of the restorations.

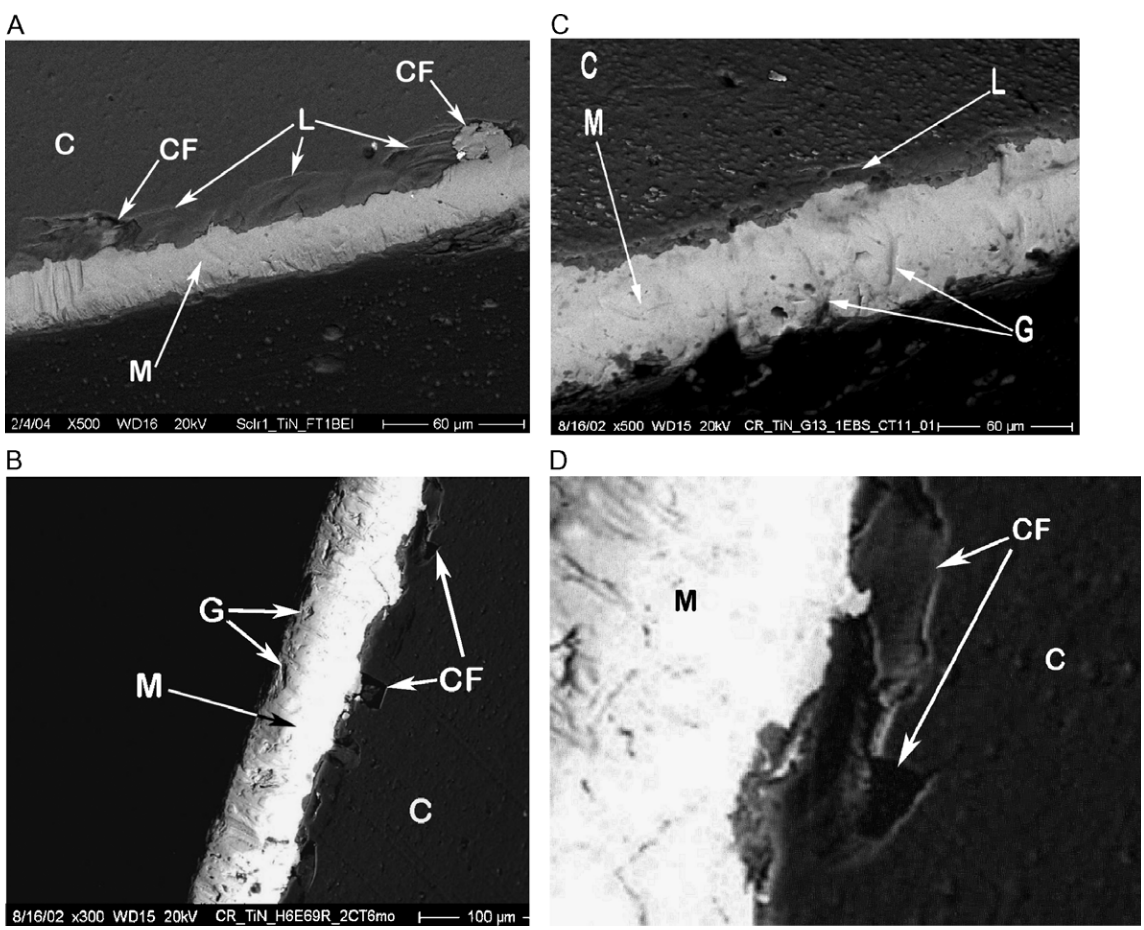

Fig. 21. Coated scalers after 3 months (A), 6 months (B) and 11 months (C) in clinical use. Magnification of edge plastic deformation (D).

5. The type of scaling the operator performs.
6. Does the operator use the scaler for any unintended uses, e.g., reshaping overhanging margins of restorations, removing orthodontic cement (an extremely abrasive material) or as a chisel during tooth preparation for placing fillings.

The BEI views of wear lands of coated scalers after 3, 6 and 11 months in clinical operation are shown in Fig. 21A, B, and C, respectively. They show coating **C** which is smooth, continuous and is totally undamaged after the clinical use, cleaning and sterilization cycles. The coating is worn in layers L adjacent to the wear land. There are occasional points of catastrophic failure CF where the substrate has undergone plastic deformation. Where the deformation was not excessive, the coating exhibits fracture lines but still remain adherent to the substrate metal. A close-up view of one of these zones is shown in Fig. 21D. The cutting edge shows a wear land with exposed metal M on the cutting edge. The gouges G are caused by heavy mechanical forces, due to the instrument's contacts with sharp restoration margins harder than stainless steel.

In clinical practice, the scalers are used basically in two modes. Supragingival scaling (scaling above the gumline) requires the scaler to withstand heavy stresses as the bulk calculus is broken off the supporting tooth material. This type of scaling also is complicated by the presence of edges or restorations. These can be

- silver–tin–mercury amalgams
- macrofilled, composite resins (filler particle size >20 μm)
- hybrid composite resins (filler particle size between 2 μm and 20 μm); the filler particles range from glass particles to zircon particles to aluminum oxide particles
- gold alloy crown margins
- nickel chromium alloy crown margins
- porcelain crown margins

All these margins are significantly harder and/or tougher than normal tooth material and in many cases harder than steel. This explains the crushing and gouging effects on the cutting edges of the instruments.

The other scaling mode is subgingival (below the gum line). This is usually done, by a dentist or a periodontist, sometimes as far as 10 or 12 mm beyond the crest of the gum. This procedure requires the scaler or curette to be impeccably sharp. Since visual observation is impossible, tactile sensing is critical. The scaler is advanced into the gum pocket in contact with the tooth surface. The sharp edge of the scaler then permits the dentist to feel the irregularities of the root. On the working stroke, the scaler engages and removes the adhering islands of calculus, rough cementum or damaged dentine. This scaling mode is ideally suited for the coated scalers. The coating insures that the edge is impeccably sharp, the finish on the scaler blade is very smooth, leaving a mirror smooth surface on the root of the tooth, and the wear mode is almost entirely abrasive, which gives the optimal performance with the coated scalers. Deep, subgingival scaling is frequently associated with a procedure known as curettage, where the blade of the scaler is directed outwards, and is used to scrape out the inflamed lining of the gum pocket. This procedure depends on the scaler's edge remaining sharp and unaffected by the scaling procedures.

When the coated scalers were used, in clinical settings, for the purposes for which they were designed, where scalers are used against tooth material, bone and/or soft tissue, they can perform for very long periods, ranging from about 3 to 6 and in some cases up to 11 months with no necessity for re-sharpening. In opposite, uncoated scalers are usually resharpened after each use or at least every few days. This, in itself, provides a great convenience and economical interest for the dentist or hygienist since two 5-min sharpening sessions could cost as much as the entire cost of the scaler in lost productivity.

The consistently smooth, sharp edge of the scaler or curette eliminates the necessity of continuous readjustment of the angle and/or pressure of the instrument on the tooth to maintain constant level of performance. The smoothness of the cutting edge reduces the risk of inadvertently producing a serrated surface of the root, which could actually promote plaque deposition and promote the progress of decay and/or periodontal disease. The absence of the microscopic metal burs, which are invariably produced during sharpening, reduces the risk of embedding irritating steel foreign body particles into an unstable, delicate gingival tissue. The true clinical significance of these factors must be further investigated.

When the scalers were grossly abused, the failure of the instruments was as a result of the catastrophic failure of the metal substrate. The coating protects the metal substrate from abrasive wear but has little capacity to protect against mechanical insults, which damage the structure of the metal substrate. Therefore, any improvement in the hardness of the metal substrate would be beneficial to the longevity of the instruments and to the extent of their use.

4. Conclusions

It has been found in laboratory and clinical testing of surface-engineered dental cutting instruments:

- Failure mode of uncoated scalers: intensive abrasive wear failure; wear land increases rapidly after the first few hundreds of strokes.
- Failure mode of coated scalers: slow, mild abrasive wear producing smooth wear areas and a decreasing wear rate until the coating is penetrated. The wear then gradually approaches that of uncoated scaler.

- LAFAD coatings of four multi-layers increase wear by 8 times.
- LAFAD coatings of eight bi-layers increase wear resistance by approximately 10 times.
- LAFAD coatings of 10 multi layers of TiN/Ti appear to increase wear resistance by at least 12.5 times.
- LAFAD coatings are resistant to tarnish and corrosion during ultrasonic cleaning and sterilizing cycles. Ultrasonic cleaning and sterilization does not affect wear resistance.
- Advanced coating architectures utilizing multiphase and nanostructured coatings as well as duplex treatment promise further increase in abrasion wear and corrosion resistance of scalers and many other dental and surgical instruments.
- The performance of the instruments in clinical practice shows more variability than under laboratory conditions. The coated instruments maintain their high-quality finish for prolonged periods of time which ranges typically in the 3–6 months range and may maintain their clinical usefulness as long as 11 months, depending on the rate of use and the operator's requirement of sharpness of the cutting edge.
- Rapid failure of the instrument is attributable primarily to the catastrophic failure of the metal structure of the scaler.
- The coating maintains its adhesion to the metal under all conditions including ultrasonic cleaning, sterilization, and clinical use and abuse. The coating does not contribute to corrosion even under adverse chemical and thermal conditions.

Acknowledgments

The study was supported in part by interact program of Material and Manufacturing Ontario (MMO). Much credit is due to Harvey Pellegrini for administrative support and valuable advice. Oleg Popov, Sergiy Molochko and Duane Jones carried out the deposition experiments. Thanks are also due to Al Deckmar for testing the instruments, D. Muechel and J. Smithers for help in sample preparation. R. Avci and P. Gannon provided electron microscopy and analysis. E. Bergmann's help in interpretation of experimental results is greatly appreciated. Fruitful discussions with D. Bhat and D. Sanders are also acknowledged.

References

[1] V. Gorokhovsky, K. Gordashnik, B. Uryukov, Proceedings of the International Ion Engineering Congress, ISIAT, vol. 83, Institute of Electrical Engineers, Kyoto, Japan, 1983.
[2] Randhava et al, US Patent No. 4,981,756.
[3] H. Brauer, Surf. Coat. Technol. 62 (1993) 618.
[4] V.I. Gorokhovsky, R. Bhattacharya, D.G. Bhat, Surf. Coat. Technol. 140 (2001) 82.
[5] V.I. Gorokhovsky, D.G. Bhat, R. Bhattacharya, A.K. Rai, K. Kulkarni, R. Shivpuri, Surf. Coat. Technol. 140 (2001) 215.
[6] V.I. Gorokhovsky, D.G. Bhat, in: I. Rajagopal, K.S. Rajam, R.V. Krishnan (Eds.), Proceedings of the GOI-UNDP International Workshop on Surface Engineering and Coatings, Bangalore (India), Allied Publishers, Ltd., Mumbai, India, 1999, p. 381.
[7] D. Sanders, R. Boxman, P. Martin (Eds.), Vacuum Arc Science and Technology, Noyes Publishing, 1995.
[8] D.G. Bhat, V.I. Gorokhovsky, R. Bhattacharya, R. Shivpuri, K. Kulkarni, Transactions of the North American Die Casting Association, 20th International Die Casting Congress and Exposition, Cleveland, OH, November 1999, 1999, p. 391.
[9] J.R. Tuck, A.M. Korsunsky, D.G. Bhat, S.J. Bull, Surf. Coat. Technol. 139 (2001) 63.
[10] W.-D. Munz, T. Hurkmans, G. Keiren, T. Trinh, J. Vac. Sci. Technol., A 11 (5) 1993 (Sep.–Oct.) 2583.
[11] H.W. Wang, M.M. Stack, S.B. Lyon, P. Hovsepian, W.-D. Munz, Surf. Coat. Technol. 126 (2000) 279.
[12] J.A. Jehn, Surf. Coat. Technol. 125 (2000) 212.
[13] E. Schafer, J. Endod. 28 (12) 2002 (December) 800.
[14] T.R. Tripi, A. Bonaccorso, G.G. Condorelli, J. Endod. 29 (2) 2003 (February) 132.
[15] J.A. Henry, R.M. Pillar, J. Biomed. Mater. Res. 58 (2) (2001) 156.
[16] H. Holleck, V. Schier, Surf. Coat. Technol. 76–77 (1995) 328.
[17] Hermann A. Jehn, Surf. Coat. Technol. 131 (2000) 433.
[18] V. Gorokhovsky, US Patent No. 6,617,057.